Egypt. J. Chem. **Vol. 64,** No. 3 pp. 1353 - 1362 (2021)

Egyptian Journal of Chemistry

http://ejchem.journals.ekb.eg/

Highly efficient capture of Th(IV) from aqueous solutions using GO/TiO_2 nanocomposite

Eman Kamal [1], **Gehad Hamdy** [2,*], **Inas. A. El-Sabbagh** [2]

[1] *Egyptian Nuclear and Radiological Regulatory Authority (ENRRA, Nasr city, Cairo, Egypt)*

[2]*Chemistry Department, Faculty of Science, Al-Azhar University (Girls, Nasr city, Cairo, Egypt)*

Abstract

An adsorbent GO/TiO_2 nanocomposite has been synthesized and characterized. FTIR, XRD, TGA, TEM, SEM and EDX were used to characterize the prepared composite. In a batch method, the adsorption properties of the prepared composite against thorium ions were examined. Th(IV) adsorption kinetics study on GO/TiO_2 suggests that the adsorption equilibrium attained within 240 min and depends on the pH value. The adsorption results were expressed mathematically by using Langmuir and Freundlich sorption models. The nanocomposite showed the highest Th(IV) adsorption of 292.32 mg/g at pH 2.5 and 25 ^oC. The thermodynamic results indicated a thermodynamically favorable, random and exothermic nature of the adsorption process. The obtained results demonstrate that GO/TiO_2 nanocomposite can be regarded as a fast, effective and convenient water-based adsorbent for adsorption of Th(IV). This study suggests that nanocomposite can be a promising candidate for the removal of Th(IV) from aqueous solution.

Keywords: Nanocomposite; Thorium; Graphene oxide; Titanium dioxide; Adsorption.

1. Introduction

Thorium as one of the normally occurring radioactive components has a wide dispersion of minor or follow sums in an enormous number of minerals. Diverse thorium applications [1], [2] produce different vaporous, fluid and strong radioactive pollutants. The characteristic radioactivity of the most inexhaustible thorium radioisotope (Th-232) and the advancement of its radioactive daughter products (Rn, Po, Bi, Ra) are the most significant restricting elements in most of thorium modern uses [3], [4]. Besides, in view of the two its radioactivity and harmfulness, thorium is a notable component to be cancer-causing and dangerous poison [5]. Subsequently, exceptional consideration has been given to remove and isolate thorium from wastewater in a conservative and safe way from the perspective of ecological assurance. The potential utilization of graphene oxide (GO) in the extraction of heavy metals [6], [7] , colored dye atoms and radionuclides from aqueous media [8]–[10] has pulled in significant enthusiasm because of its high specific surface area (hypothetical estimation of 2630 m^2/g) with lamellar structure and the presence of oxygen containing groups (hydroxyl, epoxy, carbonyl and carboxyl). Kadam et al. discovered GO membrane adsorption capacity of 380 mg/g for Cd(II) or 580 mg/g for Cu(II) at pH 4.0 when $KMnO_4$ was nine time higher than graphite [7]. Jie Li et al. indicated that the spatial element changes the particular adsorption of Th(IV) on GO from the Th(IV)/U(VI) double particle arrangement, from which we found that the interlayer separation of GO-adsorbed U(IV) was decreased contrasted with that of GO [11]. In the literature, the tendency of titanium dioxide (TiO_2) to adsorb other ions and radionuclides effectively together with thorium, cesium, strontium, fluoride and uranyl has been confirmed [1], [12]–[16]. Many studies were conducted on the evaluation of GO and TiO_2 based hybrid content in optical, catalytic, electrical and sensing purposes. However, no work has been conducted on the direction of this composite material to extract thorium or other ions within the literature. In this study, GO/TiO_2 hybrid nanocomposite was synthesized using a facile method to evaluate its ability to remove thorium from aqueous media.

2. Materials and methods

2.1. Preparation of thorium stock solution

Stock solution of thorium (1000 mg L^{-1}) was freshly prepared by dissolving specific amount of $Th(NO_3)_4.4H_2O$ (WINLAB company) in 7 ml of concentrated nitric acid (Merck company). The prepared solution was diluted to 1 liter using DI water and the desired concentration (20 – 200 mg L^{-1}) was prepared from the stock. The experimental work was carried in Safeguards analytical laboratory at the

*Corresponding author e-mail: gehadhamdy.59@azhar.edu.eg.; (Gehad Hamdy, Tel:+201008277832).

Receive Date: 03 October 2020, Revise Date: 28 November 2020, Accept Date: 06 December 2020

DOI: 10.21608/EJCHEM.2020.44957.2917

Egyptian Nuclear and Radiological Regulatory Authority (ENRRA).

2.2. Synthesis of GO/TiO₂ nanocomposite

For the synthesis of GO/TiO_2 nanocomposites (Scheme 1) 0.09 g of GO (prepared by modified Hummer' method as reported in our previous work [17]) was dispersed by sonication in 60 ml of ethanol (Sigma-Aldrich company) for 60 min, then 1.5 ml of Titanium isoperoxide ($[Ti(OCH)(CH_3)_2]_4$, Merck) was added. The resultant solution was then agitated for 30 min at room temperature. After that 0.5 ml HCl (1 M, Honeywell) and 15 ml of DI water were added dropwise with stirring the reaction at room temperature for 24 hrs. In order to remove any remaining organic traces, the sample was then centrifuged and washed with DI water. Finally, the prepared GO/TiO_2 nanocomposite dried at 80°C.

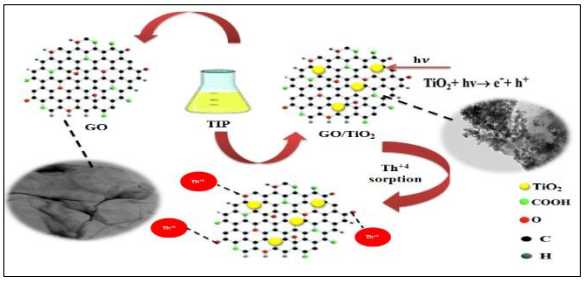

Scheme 1. The synthesis route of GO/TiO_2 nanocomposite and photocatalytic experiment.

2.3. Characterization

The crystalline nature of the prepared samples were examined using X-ray diffractometry (XRD) using wide angle X-ray scattering (Bruker axs D8, Germany, Egyptian Petroleum Research Institute) from a Cu-k_α radiation at 298 K. ATR-FTIR spectra were recorded using a Nicolet Nexus 470 spectroscope (Orion, USA, Egyptian Petroleum Research Institute), equipped with a ZnSe ATR crystal (at an incident angle of 45°). Thermal gravimetric and differential thermal analysis was acquired using (TGA 6200, SII thermogarvimetric analyzer from seiko Instrument Inc., Japan, Cairo University). Each sample was placed into aluminum crucible for measurement. Rheometric science from 20 to 1000 °C at a heating rate of 10 °C min^{-1} and a nitrogen flow of 200 mL min^{-1}. Transmission electron microscopy (TEM) was performed with JEOL (TEM-1230, Japan, National Research Center) operating at acceleration voltage of 100 kV. Samples that dispersed in deionized water were transferred to carbon coated copper grids and left to dry before testing. The surface morphology of the synthesized nano-sized composite was investigated by scanning electron microscope (SEM, JEOL6510LA, with accelerating voltage 30 kV, Japan, Egyptian Nuclear and Radiological Regulatory Authority (ENRRA). The composites were sputtered with gold before imagining. EDX detector was attached to the SEM system which used to examine the element that are present in the nanocomposite.

2.4. Batch adsorption experiment

The thorium adsorption behavior as functional of initial thorium concentration, temperature, ionic strength, pH and filtration time on the prepared nanocomposite was investigated using batch technique. Such tests were performed using 100 ml glass bottles adding different amounts of the prepared adsorbent and 20 ml of Th(IV) solution. The initial concentrations (C_0) changed in the sequence (20, 40, 80, 100, 140, 180, 200) mgL^{-1}. The glass bottles were then sonicated for 10 min, and subjected to shaking at 150 rpm at 25 °C. The solution's initial pH was modified using minimal amounts of 0.1 M HNO_3 to optimal values. To ensure that adsorbents are dispersed homogeneously in the solution and that the kinetic adsorption is complete, the solution was stirred at 150 rpm for 24 hrs. After that, the solid adsorbent was separated by filtration, and the amount of Th(IV) ions in solution was measured using inductively coupled plasma optical emission spectroscopy(ICP-OES) technique before and after adsorption process. In order to test the adsorption of thorium by glass bottle, a blank solution with the same content without any adsorbent was prepared. The thorium adsorption capacity was calculated using the following equation (1):

$$q = (C_0 - C_t)\ \mathrm{V/m} \qquad (1)$$

where q is the capacity of the adsorbent in mg/g, V the volume of the used sample in L, C_0 and C_t is the initial and final concentration of Th(IV) ion in mgL^{-1}, and m is the adsorbent weight in g.

3. Results and discussion

3.1. Characterization of GO/TiO_2 nanocomposite

The chemical compositions of the synthesized GO/TiO_2 nanocompsite were characterized by XRD and FTIR. GO was used to integrally elucidate GO/TiO_2 structure. As illustrated in Figure 1a, the GO/TiO_2 XRD patterns are well assigned to the standard rutile TiO_2 card (JCPDS 21-1276). The peak of GO which can be due to pyrolysis of high temperatures. No distinctive diffraction peaks of other phases or impurities were found in the patterns, thus suggesting the high purity of the GO/TiO_2 samples. The lattice fringes, as shown in Figure 1a, indicated that the particles are in good crystalline nature. The GO/TiO_2 nanocomposite FTIR spectra (Figure 1b) show the absorption bands corresponding to the 1050 cm^{-1} C-O stretching; 1250 cm^{-1} C-O-C stretching; 1400 cm^{-1} C-OH stretching; 1620 cm^{-1} C-C stretching; and 1720 cm^{-1} C=O carbonyl stretching [18]. They appear to be similar the GO's FTIR spectra, except for a strong FTIR band at

537.66 and 915.96 cm^{-1} is due to the Ti – O and O–Ti–C , a broad peak at 778.13 cm^{-1} corresponding to Ti–O –Ti beside all adsorption peaks of graphene oxide .That confirmed binary GO/TiO_2 nanocomposite prepared successfully, indicated that the TiO_2 was fixed in graphene sheets as a result of the strong chemical reaction between graphene oxide and TiO_2 ,also The presence of Ti–O–C bonds suggests that the −COOH moieties groups on the graphene oxide surface firmly interacted with the surface −OH groups of TiO_2 particles. Furthermore, the carboxyl group of graphene oxide could also coordinate with the titania surface through the bridging bi dentate mode Thus, TiO_2 particles were chemically bonded onto the graphene oxide surface.

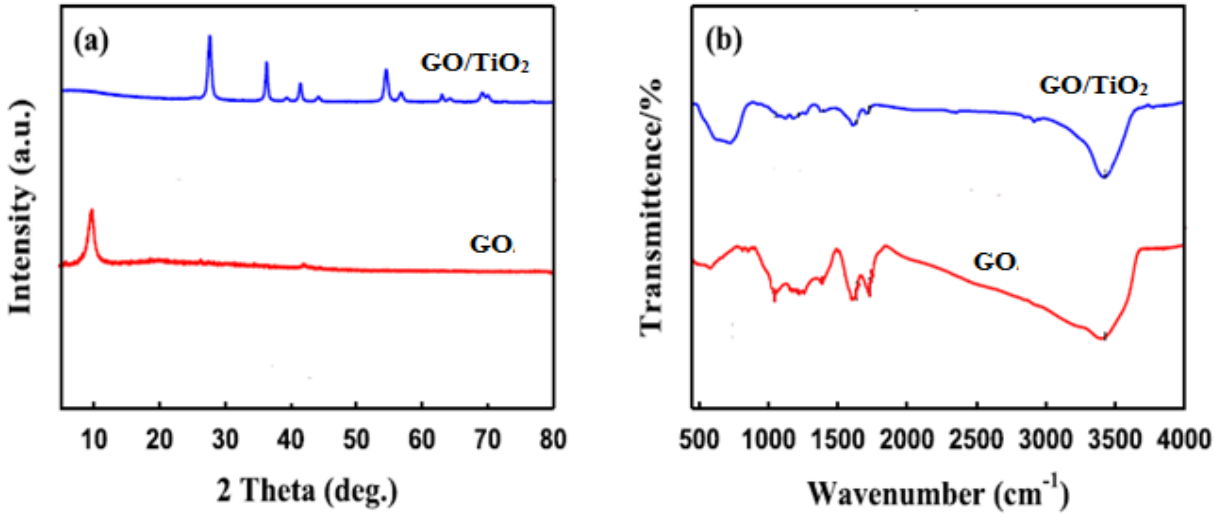

Figure 1. (a) XRD patterns of GO and GO/TiO_2 nanocomposite; (b) FTIR spectra of GO and GO/TiO_2 nanocomposite.

SEM analysis of the samples GO/TiO_2 nanocomposite was assessed. Results for the obtained nanocomposites are shown in Figure 2a. This micrograph shows the existence of TiO_2 and GO agglomerates and the latter are less visible due to the high amount of TiO_2 relative to the GO. The TiO_2 nanoparticles are also expected to adhere completely to their surfaces. The EDX result shows the present of the element C, O, and Ti in the composites being prepared (Figure 2b). TEM images further visualized the detailed morphology and microstructure of GO/TiO_2 nanocomposites as shown in Figure 2c, d. The photographs demonstrated the morphology and internal structure of the composites resulting from it. Remember that a thin nanocomposite of TiO_2 has been developed with a mean diameter about approximately 13.7 nm. Additionally, Figure 2c, suggested that a thick layer of TiO_2 was doped to the graphene particle. The TEM results obtained suggested that TiO_2 was mounted efficiently on GO sheets.

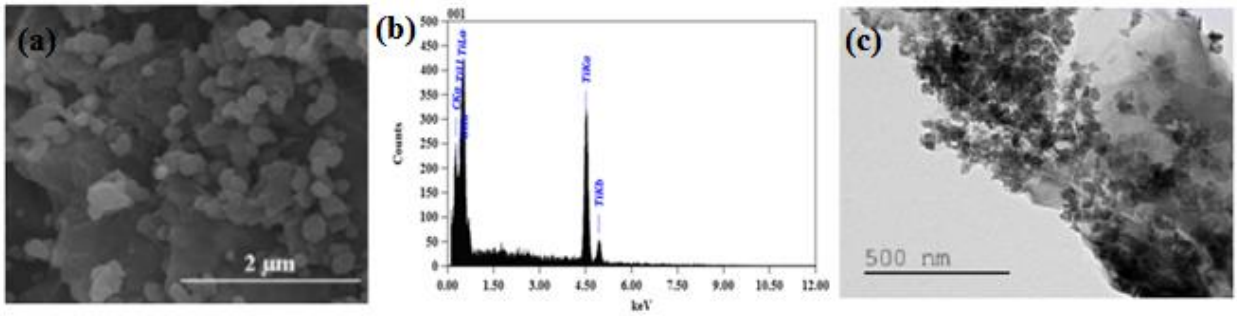

Figure 2. (a) SEM image; (b) EDX spectra and (c) TEM image of the synthesized GO/TiO_2 nanocomposite.

Another important feature which should be considered is the thermal stability of the synthesized material. A useful tool for investigating this subject is thermogravimetric analysis. This approach offers the opportunity to research the materials ' proportion and decomposition process, in addition to determining the sample stability against temperature. Figure 3 illustrates the synthesized

GO/TiO_2 nanocomposite thermogram curve, it indicated three main steps of mass change, the initial weight loss at the temperature lower than 150 °C is due to the removal of water i.e the evaporation of physisorbed and nanconfined water. The major loss of the weight at 150–300 °C, is due to the loss of functional groups with the release of CO_x species i.e the degradation of the functional groups on graphene oxide (i) H_2O release through the dehydration of the neighboring hydroxyl groups and (ii) releasing of CO and CO_2 from the decarbonation reaction [19]. Finally, the destruction of the graphene carbon skeleton occurs above 450 °C [20] that assigned to the carbon network degradation and to the removal of the most stable oxygen functionalities. From the properties of TGA thermogram it can be inferred that the existence of GO sheets in the TiO_2 matrix obviously affected the TiO_2 thermal properties.

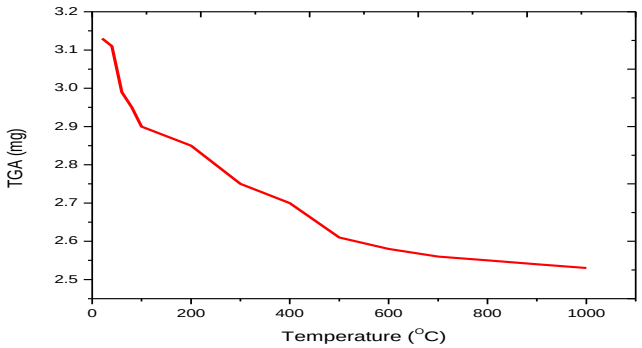

Figure 3. TGA plot of the synthesized GO/TiO_2 nanocomposite.

3.2. Thorium adsorption from its aqueous solution

Solution pH value is an important parameter which optimizes the sorption capacity due to pH affecting the metal species in solution and the ligand surface binding sites [21]. Experiments are therefore carried out to study the effect of pH on the adsorption of Th(IV) by increasing the pH from 1.5 to 4.5 and the outcomes are shown in Figure 4. As shown in Figure 4, pH is the Th(IV) adsorption controlling factor, the results demonstrate maximum sorption capacity for Th(IV) onto GO/TiO_2 nanocomposite at pH 2.5 with a removal percentage of 99.90 %. It is clear that, in acidic region, sorption is very low and as pH increases the fraction of Th(IV) adsorbed on GO/TiO_2 and the maximum adsorption is at pH 2.5. With further increasing on pH there is no change in the sorption efficiency. This observation can be interpreted at low pH values, the sorbent surface would be closely associated with H_3O^+ hydroxonium ions that compete with the positive Th(IV) ions for the adsorption sites that prevent the adsorption of metal ions to the functional surface groups. Increasing the pH value further results in decreased sorption efficiency, the functional groups on the surfaces of GO's became deprotonated and negatively charged GOs, leading to more stable GO suspensions and electrostatic attraction of GOs with Th(IV) [22]. It is found that in acidic area, the sorption of thorium ions on GO/TiO_2 nanocomposite is very small. Th(IV) adsorption improved as the pH of solution increased due to reduced competition for hydrogen ion and metal ions. To prevent blocking of GO at higher pH levels, pH 2.5 was chosen for metal uptake experiments.

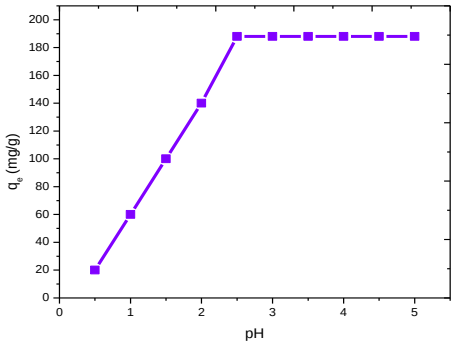

Figure 4. Effect of pH on the adsorption capacity of Th(IV) on GO/TiO_2 nanocomposite.

The effect of different salt concentration on thorium adsorption was studied in order to study the adsorption efficiency of thorium on GO/TiO_2 nanocomposite more systematically and comprehensively. Figure 5a shows the relationship between ionic strength (0.5 to 2.5 M $NaNO_3$) and thorium adsorption capacity on GO/TiO_2 nanocomposite. The results show that the adsorption of Th(IV) on GO/TiO_2 nanocomposite decreases with increasing ionic strength. This observation could be attributed to the presence of the competing cations of the salt which will reduce the adsorption. On other hand, ionic strength of a solution affected by the activity coefficient of Th(IV), which reduce its transfer

to composite surfaces [23]. So, as the ionic strength increases, a thinner double layer can be produced by the higher concentration of electrolyte ions, limiting the interaction between the adsorbent and adsorbent surfaces and decreasing adsorption [24], [25].

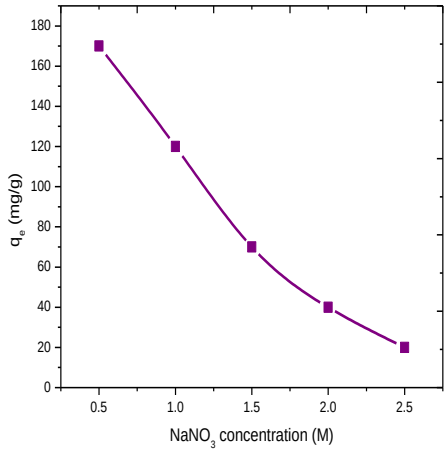

Figure 5. Effect of ionic strength on the adsorption capacity of Th(IV) on GO/TiO_2 nanocomposite (C_0 = 100 mgL^{-1} ,T=25 ^oC , pH = 2.5).

Optimum contact time was determined by varying the equilibrium time in a set of experiments where the initial concentration of Th(IV) ions, solution pH, quantity of GO/TiO_2 and temperature were kept constant. The results in Figure 5a indicated that the sorption capacity of Th(IV) on GO/TiO_2 nanocomposite increases rapidly within 10 min and reaches saturation at about 240 min. this because the adsorbent surfaces become saturated. In addition, the shift in the adsorption process of the equilibrium may be related to the gradual completion of occupation of the active adsorption sites available [26]. Additional contact time increases have no effect on the effect on the process of adsorption. Therefore, the further experiments were done by 4 h balancing with the sorbent.

3.3. Adsorption kinetics

The adsorption kinetic studies are very useful models to study of the adsorption mechanism and also provide valuable scientific and theoretical data for the construction of water treatment systems. Thus, the widely used "pseudo-first-order" and "pseudo-second-order" adsorption kinetic models were adopted in this study to evaluate the time-dependent thorium adsorption process and the method of controlling thorium adsorption mechanism. The pseudo-first - order model predicts that physical interaction regulate the adsorption mechanism while the pseudo-second - order model's proposed that chemical interaction occurs across the actual adsorption [27]. The fitting results and the corresponding parameters of thorium adsorption on GO/TiO_2 nanocomposite are shown in Figure 5b and c, respectively. Clearly, the pseudo-second - order matching better than the pseudo-first - order curves because the pseudo-second - order demonstrated higher correlation coefficients (R^2 = 0.997) indicating that the rate determining step of the thorium adsorption mechanism on GO/TiO_2 nanocomposite was chemisorption. Consequently, the adsorption mechanism will consider the interaction between thorium and the adsorbent active functional groups related to sharing of valence electron [28]. In this study, the intra - particle diffusion model was studied in order to even further illustrate the particle transfer path during the adsorption process. Figure 5d illustrates the fitting plot of q_t vs. $t^{1/2}$. As can be seen in Figure 5d, the graphs are made up of three phases and don not pass through origin point, proposing that the adsorption mechanism was not affected by single variable. In contrast, the values of diffusion rate arranged in the order $k_1 > k_2 > k_3$, demonstrating that thorium was at first adsorbed on the GO/TiO_2 outer surface. The internal saturation finally accomplished when the adsorbed thorium was eventually transferred into the interior of the GO/TiO_2 via the internal mass transfer driving force [29]. Finally, the existence of GO surface coating enhanced adsorption of thorium owing to huge number of active functional groups in the GO. The chemical initiation effect produced by the inner C-O bond promotes the expansion of adsorbed thorium on the surface coating.

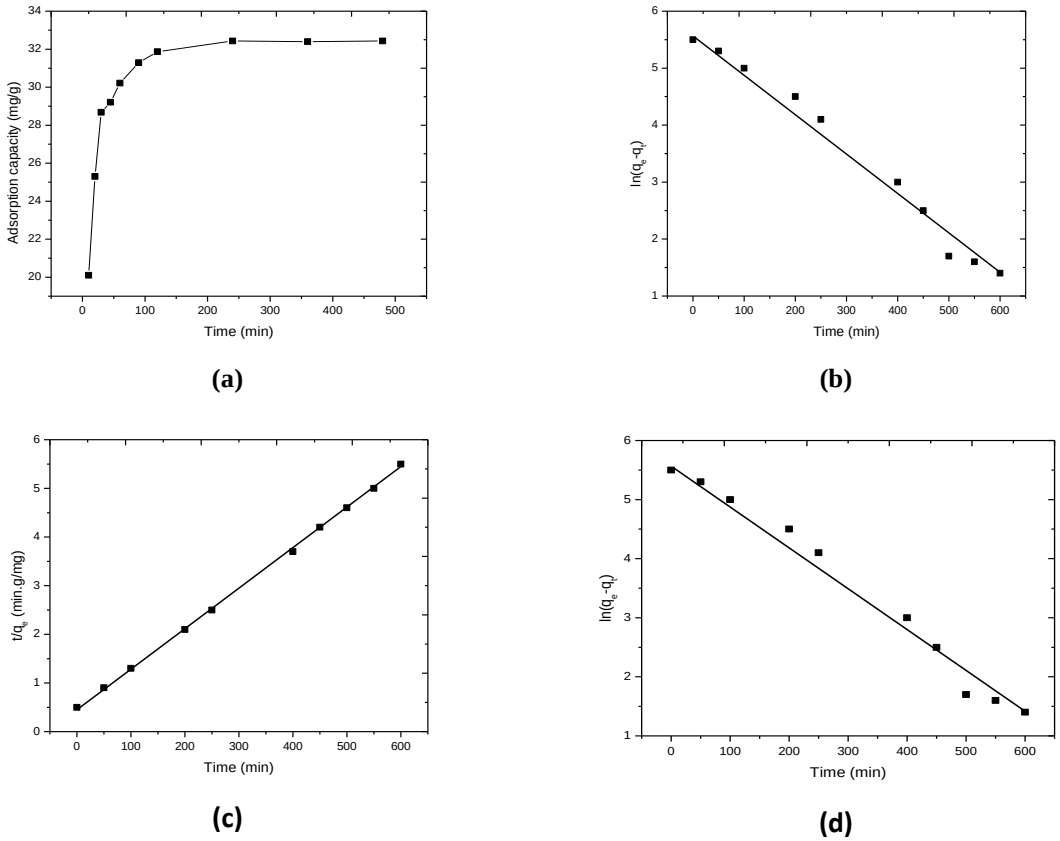

Figure 6. (a) Effect of contact time on Th(IV) adsorption by GO/TiO_2 nanocomposite, (b) pseudo-first order model, (c) pseudo- second order model and (d) intra-particle diffusion model.

3.4. Adsorption isotherm

The relationship between the quantities adsorbed by an adsorbent unit mass and the quantities of solute staying in the liquid phase at equilibrium was represented using the adsorption isotherm [30]. The effect of the initial concentration on thorium adsorption capacity was studied at different Th(IV) concentrations of 20- 200 mgL^{-1} at different temperatures from 25 to 45 ^oC. Figure 7 illustrates the impact of initial Th(IV) concentration on the thorium adsorption capacity. The results indicated that the adsorption ability of GO/TiO_2 steadily increased as the initial concentration increased until equilibrium is attained. The maximum adsorption capacity of 292.32 mg/g was obtained at an initial concentration of 100 mgL^{-1} and 25 ^oC. This pattern could be based on the assumptions that the increase in the initial concentration was accompanied by a stimulation in the concentration 's mass transfer driving force at solid-liquid interface, that may result in an increase in thorium adsorption capability on the GO/TiO_2 adsorbent [31].

Langmuir and Freundlich isotherm models were used to investigate the adsorption isotherm. The model Langmuir assumes that the adsorption process occurs on a homogeneous surface with comparable adsorption sites [32]. Langmuir isotherm's mathematical expression is given by Eq. (2):

$$\frac{C_e}{q_e} = \frac{C_e}{q} + \frac{1}{qb} \qquad (2)$$

where q_e represents the amount of solute adsorbed per unit weight of adsorbent (mg/g) at equilibrium; C_e is the equilibrium solute concentration (mg/L) in solution, q (mg/g) is the maximum monolayer adsorption and b (L/mg) the Langmuir constants that used to investigate the energy of adsorption and correlated to the affinity of binding sites. On other hand, the Freundlich model (empirical model) is based on the assumption that the adsorption process is multilayer adsorption on a heterogeneous surface [33] and can be expressed by Eq. (3):

$$\log q_e = \log k_F + \frac{1}{n}\log C_e \qquad (3)$$

where k_F and n are the Freundlich constants, which represent adsorption capacity and adsorption intensity, respectively. Figure 8a and b indicate the Th(IV) adsorption isotherm data fitting to the Langmuir and Freundlich isotherm models. The Langmuir plot R^2 value is (0.997) and the equilibrium constant is 0.029 L/mg. The estimated maximum theoretical capacity 250.59 mg/g. Whereas Freundlich's R^2 value is

(0.985) and k_F constant is 54.21. In the study, the Langmuir equation, based on the correlation coefficients, provides a better fit of experimental data for Th(IV) adsorption over the entire concentration range than the Freundlich. This observation suggests the homogeneity of Th(IV) adsorption on the GO/TiO_2 nanocomposite assembling with monolayer adsorption formation.

The results above indicate that the thorium adsorption process on the GO/TiO_2 was likely on specific homogeneous functional sites within the GO/TiO_2, i.e., thorium formed a uniformly distributed monolayer on the GO/TiO_2 surface and was captured using s site-to-site adsorption mechanism by related functional groups (such as carbonyl, epoxy and carboxyl groups). In conclusion, the lower coefficients of the Freundlish models showed that chemisorption accompanied by physical adsorption dominated the thorium adsorption process.

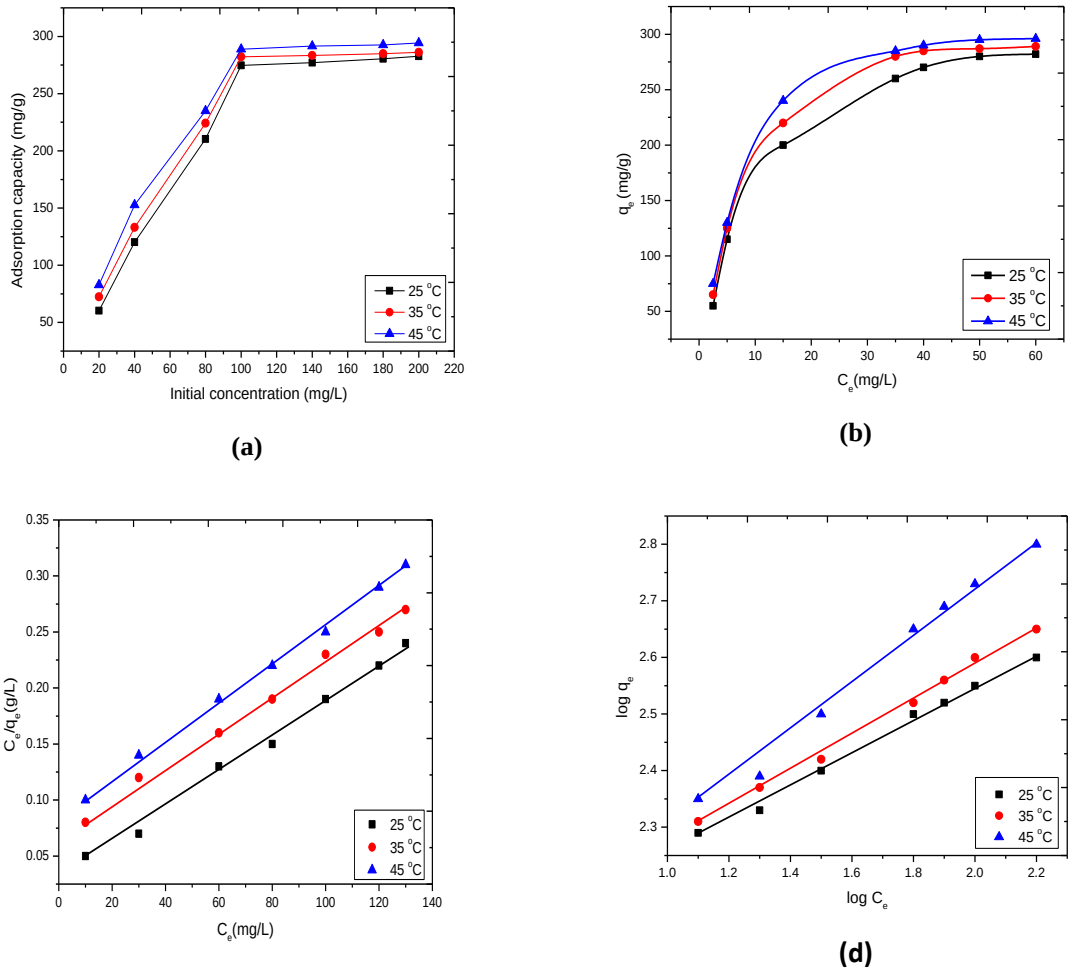

Figure 7. (a) Effect of initial Th(IV) concentration on its adsorption by GO/TiO_2 nanocomposite, (b, c) Langmuir and (d) Freundlish isotherm models.

3.5. Thermodynamic studies

The influence of temperature for thorium adsorption capacity on GO/TiO_2 adsorbent is studied in the temperature ranges from 25 to 45 ºC, while all other variables have been held constant at their optimum values. The results were observed (Figure 8) appear to suggest that, with rising temperature, the thorium adsorption capacity decreased, proposing that the process was exothermic one. Equation 4 can be used to examine the thermodynamic properties such as enthalpy change ΔH (kJ/mol) and entropy change ΔS (kJ/(mol K)) for Th(IV) adsorption on GO/TiO_2 nanocomposite:

$$\ln K_d = \frac{\Delta S^o}{R} - \frac{\Delta H^o}{RT} \qquad (4)$$

Where K_d is distribution coefficient, R (8.314 J/mol K) is the universal gas constant, T is the temperature in Kelvin. It is possible to determine the standard free energy change ΔGº from the next equation Eq. (5):

$$\Delta G^o = T\Delta H^o - \Delta S^o \qquad (5)$$

Figure 8b represents the relations between ln K_d vs 1/T for thorium adsorption on GO/TiO_2 nanocomposite and the evaluated thermodynamic variables are indicated in Table 1. The negative value of ΔH for thorium adsorption illustrates that thorium adsorption on GO/TiO_2 nanocomposite is an exothermic operation. The assumption that the enthalpy is negative is in accordance with the finding that the thorium adsorption on GO/TiO_2 nanocomposite is decreased by temperature increases. Thorium's adsorption positive ΔS^o reflects that the spontaneity of the adsorption mechanism. While the negative ΔG^o values confirm the spontaneous nature for the thorium adsorption on GO/TiO_2 nanocomposite. On other hand, the values of ΔG^o which increase with increasing temperature illustrating that there is a higher degree of spontaneity at higher temperature [34]. The thermodynamic variables explained that in aqueous solutions there are certain structural changes in the GO/TiO_2 nanocomposite adsorbents that influence their affinity to thorium ions[35].

Table 1: Thermodynamic parameters of Th(IV) adsorption

GO/TiO_2 nanocomposite					
ΔH (kJ/mol)	**ΔS (J/mol K)**	**ΔG(kJ/mol)** 298.1K	303.1K	308.1	**313.1**
-84.14	288.3	-86.02	-87.46	-88.90	**-90.35**

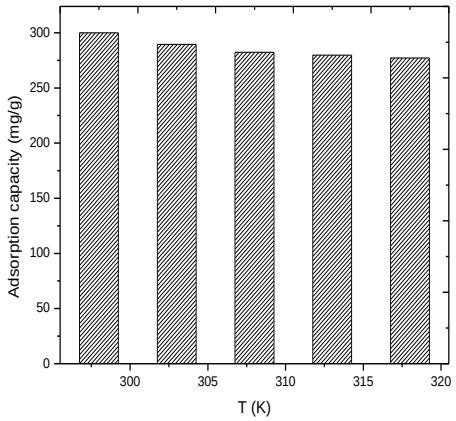

(a)

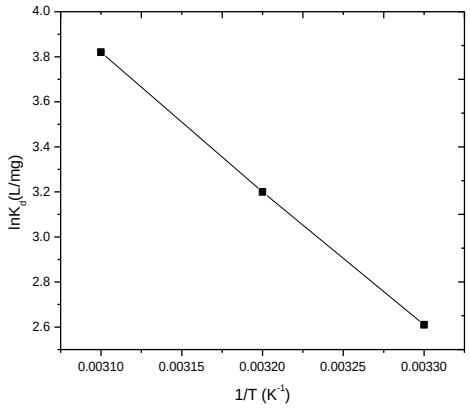

(b)

Figure 8. Effect of temperature on (a) adsorption capacity and (b) K_d of thorium.

ACKNOWLEDGMENT

Great thanks to Egypt Nuclear & Radiological Regulatory Authority (ENRRA) for supported ICP-OES Instrument.

4. Conclusion

In this study, the GO/TiO_2 nanocomposite was prepared for the removal the Th(IV) ions from aqueous media. It demonstrated an excellent Th(IV) adsorption capacity equal to 292.32 mg/g at pH 2.5 and 25 ^oC. The adsorption process of Th(IV) on GO/TiO_2 nanocomposite was independent on ionic strength and dependent on pH. The kinetics study suggested that the adsorption process of Th(IV) on GO/TiO_2 nanocomposite was fitted well by pseudo-second-order kinetic model, and the thermodynamic study that the adsorption process of Th(IV) fitted with Langmuir models. Meanwhile, it was a typical spontaneous and exothermic reaction based on the values of ΔH^o, ΔG^o and ΔS^o. These results indicated that GO/TiO_2 nanocomposite were a promising adsorbent, which was possible to be candidate for the removal of actinides ions from wastewater in the future.

References

[1] Y. Khazaei, H. Faghihian, and M. Kamali, "Removal of thorium from aqueous solutions by sodium clinoptilolite," *J. Radioanal. Nucl. Chem.*, 2011.

[2] B. W. Jordan, R. G. Eggert, B. W. Dixon, and B. W. Carlsen, "Thorium: Crustal abundance, joint production, and economic availability," *Resour. Policy*, 2015.

[3] Z. W. Huang, Z. J. Li, L. R. Zheng, W. S. Wu, Z. F. Chai, and W. Q. Shi, "Adsorption of Eu(III) and Th(IV) on three-dimensional graphene-based macrostructure studied by spectroscopic investigation," *Environ. Pollut.*, 2019.

[4] M. Shahin, sayed Elmongy, E. Saad, A. Shazly, and A. Ezzat, "Evaluation of Rare Earth Elements in Black Sand and Phosphate ores, EGYPT," *Egypt. J. Chem.*, 2020.

[5] Y. Hu *et al.*, "Selective separation and preconcentration of Th(iv) using organo-functionalized, hierarchically porous silica monoliths," *J. Mater. Chem. A*, 2019.

[6] L. Liu *et al.*, "Adsorption of Au(III), Pd(II), and Pt(IV) from aqueous solution onto graphene oxide," *J. Chem. Eng. Data*, 2013.

[7] P. Tan *et al.*, "Adsorption of Cu2+, Cd2+ and Ni2+ from aqueous single metal solutions on graphene oxide membranes," *J. Hazard. Mater.*, 2015.

[8] J. Zhao, Z. Wang, J. C. White, and B. Xing, "Graphene in the aquatic environment: Adsorption, dispersion, toxicity and transformation," *Environ. Sci. Technol.*, 2014.

[9] H. Yan *et al.*, "Influence of the surface structure of graphene oxide on the adsorption of aromatic organic compounds from water," *ACS Appl. Mater. Interfaces*, 2015.

[10] D. Jiang *et al.*, "The separation of Th(IV)/U(VI) via selective complexation with graphene oxide," *Chem. Eng. J.*, 2015.

[11] J. Li *et al.*, "Removal of Cu(II) and fulvic acid by graphene oxide nanosheets decorated with Fe 3O 4 nanoparticles," *ACS Appl. Mater. Interfaces*, 2012.

[12] C. E. Yılmaz, M. A. A. Aslani, and C. K. Aslani, "Removal of thorium by modified multi-walled carbon nanotubes: Optimization, thermodynamic, kinetic, and molecular dynamic viewpoint," *Prog. Nucl. Energy*, 2020.

[13] M. Hua, S. Zhang, B. Pan, W. Zhang, L. Lv, and Q. Zhang, "Heavy metal removal from water/wastewater by nanosized metal oxides: A review," *Journal of Hazardous Materials*. 2012.

[14] S. Li, L. Wang, J. Peng, M. Zhai, and W. Shi, "Efficient thorium(IV) removal by two-dimensional Ti2CTx MXene from aqueous solution," *Chem. Eng. J.*, 2019.

[15] X. Yang *et al.*, "Removal of thorium and uranium from leach solutions of ion-adsorption rare earth ores by solvent extraction with Cextrant 230," *Hydrometallurgy*, 2020.

[16] A. Youssef, E. Nabil, and N. Mahmoud, "Influence of polymers loaded with ZnO and TiO2 nanoparticles on thermal resistance of archaeological Wood," *Egypt. J. Chem.*, 2020.

[17] M. Fathy, A. Gomaa, F. A. Taher, M. M. El-Fass, and A. E.-H. B. Kashyout, "Optimizing the preparation parameters of GO and rGO for large-scale production," *J. Mater. Sci.*, vol. 51, no. 12, 2016.

[18] E. S. Aziman, A. H. J. Mohd Salehuddin, and A. F. Ismail, "Remediation of Thorium (IV) from Wastewater: Current Status and Way Forward," *Sep. Purif. Rev.*, 2019.

[19] F. Wang and K. Zhang, "Reduced graphene oxide-TiO2 nanocomposite with high photocatalystic activity for the degradation of rhodamine B," *J. Mol. Catal. A Chem.*, 2011.

[20] A. Tayel, A. R. Ramadan, and O. A. El Seoud, "Titanium dioxide/graphene and titanium dioxide/graphene oxide nanocomposites: Synthesis, characterization and photocatalytic applications for water decontamination," *Catalysts*. 2018.

[21] M. A. Mahmoud, A. Abutaleb, I. M. H. Maafa, I. Y. Qudsieh, and E. A. Elshehy, "Synthesis of polyvinylpyrrolidone magnetic activated carbon for removal of Th (IV) from aqueous solution," *Environmental Nanotechnology, Monitoring and Management*. 2019.

[22] A. Nilchi, T. Shariati Dehaghan, and S. Rasouli Garmarodi, "Kinetics, isotherm and thermodynamics for uranium and thorium ions adsorption from aqueous solutions by crystalline tin oxide nanoparticles," *Desalination*, 2013.

[23] T. S. Anirudhan, P. S. Suchithra, P. Senan, and A. R. Tharun, "Kinetic and equilibrium profiles of adsorptive recovery of thorium(IV) from aqueous solutions using poly(methacrylic acid) grafted cellulose/bentonite superabsorbent composite," *Ind. Eng. Chem. Res.*, 2012.

[24] J. Zhou *et al.*, "Highly selective and efficient removal of fluoride from ground water by layered Al-Zr-La Tri-metal hydroxide," *Appl. Surf. Sci.*, 2018.

[25] X. H. Xiong *et al.*, "Selective extraction of thorium from uranium and rare earth elements using sulfonated covalent organic framework and its membrane derivate," *Chem. Eng. J.*, 2020.

[26] X. Zhang, X. Lin, Y. He, Y. Chen, J. Zhou, and X. Luo, "Adsorption of phosphorus from slaughterhouse wastewater by carboxymethyl konjac glucomannan loaded with lanthanum," *Int. J. Biol. Macromol.*, 2018.

[27] H. Ding, X. Zhang, H. Yang, X. Luo, and X. Lin, "Highly efficient extraction of thorium from aqueous solution by fungal mycelium-based microspheres fabricated via immobilization," *Chem. Eng. J.*, 2019.

[28] X. Wang *et al.*, "The synergistic elimination of uranium (VI) species from aqueous solution using bi-functional nanocomposite of carbon sphere and layered double hydroxide," *Chem. Eng. J.*, 2018.

[29] A. Rahmani-Sani, A. Hosseini-Bandegharaei, S. H. Hosseini, K. Kharghani, H. Zarei, and A.

Rastegar, "Kinetic, equilibrium and thermodynamic studies on sorption of uranium and thorium from aqueous solutions by a selective impregnated resin containing carminic acid," *J. Hazard. Mater.*, 2015.
[30] I. Liatsou, E. Christodoulou, and I. Pashalidis, "Thorium adsorption by oxidized biochar fibres derived from Luffa cylindrica sponges," *J. Radioanal. Nucl. Chem.*, 2018.
[31] S. M. Yakout, "Influence of solution chemistry on the selective adsorption of uranium and thorium onto activated carbon," *Nucl. Technol.*, 2015.
[32] T. A. Saleh, A. Sari, and M. Tuzen, "Chitosan-modified vermiculite for As(III) adsorption from aqueous solution: Equilibrium, thermodynamic and kinetic studies," *J. Mol. Liq.*, 2016.
[33] Z. Han, Z. Tang, S. Shen, B. Zhao, G. Zheng, and J. Yang, "Strengthening of Graphene Aerogels with Tunable Density and High Adsorption Capacity towards Pb 2+," *Sci. Rep.*, 2014.
[34] A. Hosseini-Bandegharaei *et al.*, "Thorium removal from weakly acidic solutions using titan yellow-impregnated XAD-7 resin beads: kinetics, equilibrium and thermodynamic studies," *J. Radioanal. Nucl. Chem.*, 2016.
[35] D. Baybaş and U. Ulusoy, "The use of polyacrylamide-aluminosilicate composites for thorium adsorption," *Appl. Clay Sci.*, 2011.

الملخص العربى

فصل عالى الكفاءة للثوريوم الرباعى من المحاليل المائية بإستخدام المتراكب النانوى أكسيد الجرافين المطعم بأكسيد التيتانيوم

يهدف البحث إلي تحضير مواد مركبة نانومترية جديدة محتوية فى تركيبها الاساسي علي اكسيد الجرافين المركب الثنائى GO/TiO_2 واستخدام هذا المركب النانووى لإزالة الثوريوم الرباعي من المحاليل المائية دون حدوث أى تأثير سلبي على الصحة والبيئة.

تم توصيف المواد المركبة والمواد الأساسية بإستخدام التحليل الطيفي بالأشعة تحت الحمراء"IR" ، حيود الأشعه السينية "XRD" ، صور المجهر الإلكتروني بالماسح الضوئي"SEM " ، التحليل الطيفي بتشتيت الطاقة بالأشعة السينية"EDX" ،صور المجهر الإكترونى النافذ "TEM") لمعرفة أشكال ، تركيب ودرجة نقاوة هذة المواد المركبة الجديدة وكذا دراسة الثبات الحرارى لهذه المواد بإستخدام جهازالتحليل الوزن الحرارى.

وقد تم تطبيق المركب الثنائى GO/TiO_2 لإزالة الثوريوم من المحاليل المائية عن طريق الدفعة الواحدة الثابتة تحت تأثير العوامل التجريبية المختلفة مثل دراسة تأثيرالتركيز الإبتدائى للثوريوم الرباعى و درجة الحموضة والقلوية للمحلول (الأس الهيدروجينى) و تأثير درجة الحرارة و الزمن و حجم المادة المركبة المستخدم و تأثير المركب الايونى فى المحلول لبيان الظروف المثالية لعملية الإزالة. كما تمت دراسة توصيف توازن الإدمصاص وحركية التفاعل والتغير فى المحتوى الحرارى لتحديد كفاءة هذة المواد الجديدة لإزالة الثوريوم الرباعى. كما تمت دراسة مدى ثبات وإعادة إستخدام المواد المركبة النانومترية الجديدة وكذا استرجاع الثوريوم المدمص وإعادة إستخدام المادة المركبة مرة أخرى.

وقد أوضحت دراسة العوامل التجريبية المختلفة أن المتراكب النانووى المحضر له القدرة على فصل الثوريوم من المحاليل المائية بنسبة تصل إلى 99.7% وسعة إدمصاص تعادل 32.361 مجم/جم.

تم تطبيق المواد المتراكبة قيد الدراسة على إزالة كل من عنصري اليورانيوم والانثانوم مع الإحتفاظ بكافة الظروف التجريبية المثالية. وتبين من الدراسة قدرة هذا المتراكب الجديد على إزالة اليورانيوم بنسبة 98% تقريبا لكلا المركبين بينما إزالة الأنثانوم لم تتجاوز نسبة 30%.

وختاما يتبين من الدراسة أن المتراكب النانووى الجديد GO/TiO_2 له كفاءة عالية لإزالة عنصر الثوريوم الرباعى من المحاليل المائية دون حدوث أى تأثير سلبي على الصحة العامة والبيئة. كما تبين المتراكب المحضر له ثبات عالى . ويمكن إسترجاع الثوريوم مرة أخرى وإستخدام المركبات مجددا لما فى ذلك قيمة إقتصادية. وبلذلك يمكن القول أن هذا المتراكب يمكن إستخدامه بيئيا للتحكم فى التلوث النووى الصناعى وكما يمكن استخدامها بغرض التحقق فى أعمال الضمانات النووية .